Some Results for Thin-Iris Loaded Periodic Waveguides

D. ROSENBERG, MEMBER, IEEE, AND D. J. R. STOCK, ASSOCIATE MEMBER, IEEE

Abstract—The planar waveguide holding planar obstacles is a prototype structure—its fields correspond to some sets of lowest modes in circular and coaxial line waveguides that use coaxial iris loading and in inductive iris loaded rectangular guides. An analysis of a periodically thin-iris loaded planar waveguide is offered, the procedure for which can also be applied to the other waveguides mentioned. A particular example for small iris separation is considered. Among the results of this study are adjustments to some formulas of Brillouin so as to allow consideration of large phase shifts per cell of periodic guide. The procedure, which can be recommended as a formula deriving technique, can find use with such other planar obstacles as the thick periodic iris, the interdigitally placed irises, or the single iris in a multimode guide. Some consideration is given to interdigital loading.

I. Introduction

THE SYMMETRIES of waveguide obstacles are useful when they can divide the set of normal modes into sufficiently small, distinct subsets. They are further useful when several types of guide fall together as a class because of similar symmetry properties. The following guides, because of the planar obstacles they hold, form such a class; namely, such irises in the planar waveguide, coaxial irises in the circular waveguide or in the coaxial line waveguide, and inductive window irises in rectangular waveguides. In all of these cases, there is a distinctive subset of normal modes which includes some modes of the lowest order.

By treating only obstacles in the planar waveguide, one obtains a prototype of analysis for the remaining cases mentioned. Hence the planar guide, with periodically arrayed thin irises (as shown in Fig. 1), will be considered here. Two points are worth noting beforehand as important to the analysis. On the one hand, an appropriate series representation of the field operator will be employed. On the other hand, use will be made of a simplified interpretation of elements of the series of operators. It will be plain how the procedure can be extended to cover the cases of other waveguides mentioned.

Among the results will be some relations for adjusting the formulas of earlier studies[1,2,3] of this periodic guide configuration for the sake of extending the range of possible phase shift per section. It is thought, because of the attention given to accuracy, that the results will be useful for representation of such multimode guides. The emphasis of what follows is upon method (upon its formal display, at least), and this is reflected in the presence of a somewhat large section of developmental discussion.

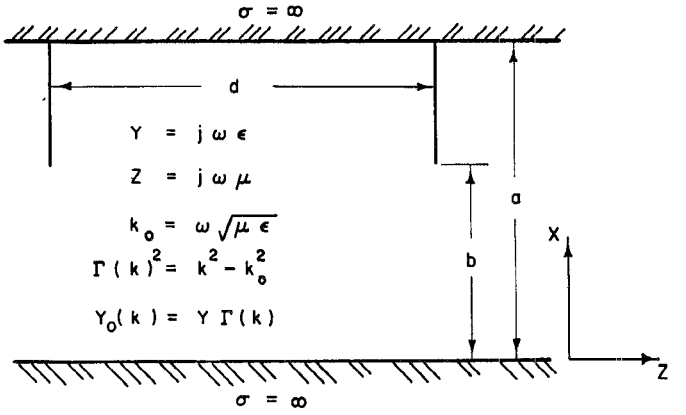

Fig. 1. Properties of the periodic loading and of the planar waveguide when E waves and the TEM wave are present. For H waves, let $Y_0(k)=Z^{-1}\Gamma(k)$.

In order to maintain simplicity, only the combined E and TEM waves are treated, although some similarly obtained results for H waves will be presented. An application of results to interdigital lines will also be shown.

II. Theoretical Characterization of the Problem

Transverse fields in each cell of the periodic guide can be given by the collection of their component normal modes. Thus, let

$$[\boldsymbol{E}_\tau(k) = \boldsymbol{E}_{\tau 0}(k)\cosh\Gamma(k)z + Z_0(k)\boldsymbol{H}_{\tau 0}(k)\times\hat{z}\sinh\Gamma(k)z] \quad (1)$$

and

$$[\boldsymbol{H}_\tau(k) = \boldsymbol{H}_{\tau 0}(k)\cosh\Gamma(k)z + \hat{z}\times Y_0(k)\boldsymbol{E}_{\tau 0}(k)\sinh\Gamma(k)z] \quad (2)$$

show a mode of the periodic guide as a vector column indexed by the wave numbers k. The notations $\boldsymbol{E}_\tau=[\boldsymbol{E}_\tau(k)]$, $\boldsymbol{H}_\tau=[\boldsymbol{H}_\tau(k)]$, $\boldsymbol{E}_{\tau 0}=[\boldsymbol{E}_{\tau 0}(k)]$, and $\boldsymbol{H}_{\tau 0}=[\boldsymbol{H}_{\tau 0}(k)]$ are a helpful convenience for handling (1) and (2). If $\mathbf{K}=[k]$ is a diagonal matrix of the wave numbers k, then one can make further convenience of the notations $Z_0(\mathbf{K})=[Z_0(k)]$, $Y_0(\mathbf{K})=[Y_0(k)]$, or

Manuscript received April 21, 1965; revised December 1, 1965. The work reported in this paper was sponsored by the U. S. Army Research Office (Durham) under Grant DA-ARO(D)-31-124-G462.

D. Rosenberg is with the University of Tennessee, Knoxville, Tenn. He was formerly with New York University, New York, N. Y.
D. J. R. Stock is with New York University, New York, N. Y.

[1] L. Brillouin, "Wave guides for slow waves," *J. Appl. Phys.*, vol. 19, pp. 1023-1041, November 1948.
[2] J. R. Pierce, *Traveling Wave Tubes*. New York: Van Nostrand, 1950.
[3] S. A. Schelkunoff and H. T. Friis, *Antennas: Theory and Practice*. New York: Wiley, 1952.

$\Gamma(\mathbf{K}) = [\Gamma(k)]$; or other scalar functions of $\mathbf{K}$. Thus, (1) has the alternate representation $E_\tau = \cosh\ \Gamma(\mathbf{K})zE_{\tau 0} + Z_0(\mathbf{K})\ \sinh\ \Gamma(\mathbf{K})zH_{\tau 0} \times \hat{z}$. Finally, where only passing interest will be the case, the collection of wave numbers k might form a continuously (as well as discretely) infinite set, depending on the guide dimensions.

If (1) and (2) are to be a mode of the periodic guide, they must fit the boundary conditions of continuity on the iris holes, zero transverse electric field on iris metal, and the amplitude variation e^{hd} from cell to cell. The corresponding constraining statements upon (1) and (2) can be put as

$$\begin{aligned} \hat{z} \times \boldsymbol{H}_{\tau 0} &= Y_i(\mathbf{K})\boldsymbol{E}_{\tau 0} \\ &= Y_0(\mathbf{K})(\coth\ \Gamma(\mathbf{K})d - e^{hd}\ \mathrm{csch}\ \Gamma(\mathbf{K})d)\boldsymbol{E}_{\tau 0} \end{aligned} \tag{3}$$

and as

$$\begin{aligned} \boldsymbol{J}_{s0} &= 2Y_l(\mathbf{K})\boldsymbol{E}_{\tau 0} \\ &= 2Y_0(\mathbf{K})(\coth\ \Gamma(\mathbf{K})d - f\ \mathrm{csch}\ \Gamma(\mathbf{K})d)\boldsymbol{E}_{\tau 0}. \end{aligned} \tag{4}$$

In (3), $Y_i(\mathbf{K})$ is a matrix of image admittances for the normal modes, looking along $z>0$, from the point $z=0^+$. In (4), $\boldsymbol{J}_{s0}$ is the field of total current density on the iris plane at $z=0$, and $2Y_l(\mathbf{K})$ is a matrix of shunt loadings for the normal modes at the iris planes. For convenience,

$$f = \cosh\ hd, \tag{4a}$$

where h is the propagation constant per cell along $z>0$.

$\boldsymbol{E}_{\tau 0}$ is normal to the iris edge. It is well known that such fields follow an inverse square root of distance law, so that $\boldsymbol{E}_{\tau 0}$ is not made of a square integrable function on the iris hole. So as to enjoy a path of least action, when a norm for $\boldsymbol{E}_{\tau 0}$ is needed, the definition

$$\|\boldsymbol{E}_{\tau 0}\|_1 = \int_0^b |\ E(x)\ |\ dx$$

will be used. This assumes $\boldsymbol{E}_{\tau 0} = \hat{x}E(x)$.

Introduce now the projection operator $\mathbf{P}$, which is such that

$$\mathbf{P}\boldsymbol{F}_\tau = \boldsymbol{F}_\tau$$

when $\boldsymbol{F}_\tau$ is a field having the value zero on iris metal, and is such that

$$\mathbf{P}\boldsymbol{F}_\tau = 0$$

when the value of $\boldsymbol{F}_\tau$ is zero over the iris hole. Thus, more generally, if $\boldsymbol{F}_\tau$ is an arbitrary field on the uniform guide cross section, $\mathbf{P}\boldsymbol{F}_\tau$ can be said to be $\boldsymbol{F}_\tau$ projected on the iris hole. $\mathbf{P}$ has the property $\mathbf{P}^t = \mathbf{P}$, where $t = 1, 2, 3, \cdots$. Although $\mathbf{P}$ can be defined well enough to work with, it has no inverse, for it is usually impossible to reconstruct the iris metal component of $\boldsymbol{F}_\tau$, given $\mathbf{P}\boldsymbol{F}_\tau$. That component is in the null space of $\mathbf{P}$. $\mathbf{P}$ has the important properties of being real and symmetrical. Thus

$$\mathrm{Re}\ \mathbf{P} = \mathbf{P} = \mathbf{P}^* = \mathrm{Re}\ \mathbf{P}^*.$$

The projector complementary to $\mathbf{P}$, which projects on iris metal, can be found from $\mathbf{P}$ as

$$\mathbf{Q} = 1 - \mathbf{P}.$$

In the problem at hand, one makes use of $\mathbf{P}$ and $\mathbf{Q}$ in the relations $\mathbf{P}\boldsymbol{E}_{\tau 0} = \boldsymbol{E}_{\tau 0}$ and $\mathbf{Q}\boldsymbol{J}_{s0} = \boldsymbol{J}_{s0}$.

That a field satisfy both (3) and (4) is necessary for solution of the periodic guide problem. These statemenst derive from the boundary conditions. More generally, an arbitrary $\boldsymbol{E}_{\tau 0}$ inserted into (3) will always yield $\boldsymbol{E}_\tau$ and $\boldsymbol{H}_\tau$ that fit Floquet's theorem, although not usually fitting boundary conditions. On the other hand, if $\boldsymbol{E}_{\tau 0}$ is such that

$$0 = \mathbf{P}Y_l(\mathbf{K})\mathbf{P}\boldsymbol{E}_{\tau 0}, \tag{5}$$

boundary conditions are automatically satisfied; and Floquet's theorem fits by use of (3). Thus, assuming (3), (5) is sufficient, as well as necessary, for $\boldsymbol{E}_{\tau 0}$ to solve the periodic iris-loaded waveguide problem.

A useful alternative to (5) can be seen in the statement

$$0 = \mathbf{Q}Z_l(\mathbf{K})\mathbf{Q}\boldsymbol{J}_{s0}, \tag{6}$$

where $Z_l(\mathbf{K}) = Y_l(\mathbf{K})^{-1}$. Since $Y_0(\mathbf{K}) = Y\Gamma(\mathbf{K})^{-1}$, when the E plus TEM combined waves are considered, one sees that (5) makes use of a bounded operator, whereas $Z_l(\mathbf{K})$ in (6) is unbounded. Were H waves being considered, it would be (6) that held the bounded operator, and (5) the unbounded $Y_l(\mathbf{K})$.

III. Further Definitions and Formulations

Because there will be much formal manipulation of operators and vectors in the subsequent discussion, it is worthwhile to show the means by which representations are made with some care, the better to trace their properties. Therefore, consider the following definitions, some of which have already been used.

First assume $\{t$: non-negative integers$\}$. Some useful subsets of $\{t\}$ are $\{t_0$: odd positive integers$\}$ and $\{t_e$: even non-negative integers$\}$.

From $\{t\}$ construct $\{k = t\pi/a\}$, which is the set of wave numbers for the given unobstructed planar waveguide. Also define the construction of $\{l = t\pi/b\}$, the wave numbers of a smaller uniform planar waveguide. Note the additional sets $\{m = t\pi/d\}$, $\{m_0 = t_0\pi/d\}$, and $\{m_e = t_e\pi/d\}$, their interpretation as waveguide wave numbers being in this case superfluous since they will be used as summation indices.

$\{k\}$ has already been used to provide indices of the coefficients used for the Fourier series representation of a field. Thus, for example, $\boldsymbol{E}_\tau = [\boldsymbol{E}_\tau(k)]$ must suggest identity between the field given by its Fourier coefficients and given by the set of its functional values on the larger waveguide cross section. A similar use can be made of $\{l\}$ for fields on the smaller waveguide cross section. In particular, if $\mathbf{P}\boldsymbol{E}_\tau = \boldsymbol{E}_\tau$, one has the relation $\boldsymbol{E}_\tau = [\boldsymbol{E}_\tau(k)] = [\boldsymbol{E}_\tau(l)]$.

Let $\alpha=\alpha\mathbf{I}$ be called a scalar operator, where $\mathbf{I}$ is the identity operator and α is a number. Thus, in a conventional way, an expression is operator or scalar depending on the terms other than α that may occur.

The diagonal operator $\mathbf{K}$ has been introduced previously as a construction from $\{k\}$. The operator $\mathbf{L}$ from $\{l\}$ can be defined similarly. $\mathbf{K}$ and $\mathbf{L}$ are not invertible since zero is a diagonal element of each of them. However, if $\alpha\neq 0$, $\mathbf{K}+\alpha$ and $\mathbf{L}+\alpha$ are invertible.

$\mathbf{K}^2$ can be identified with the operation $-\partial^2/\partial x^2$ on functions in the interval $0\leq x\leq a$, having zero derivatives at $x=0$ and $x=a$. Recall that E wave and TEM wave normal modes fit these boundary conditions. $\mathbf{K}^2$ is not invertible, but $\mathbf{K}^2-k_0^2=-\partial^2/\partial x^2-k_0^2$ is. Thus, working either with function or with sequence representations, a one dimensional wave equation can be solved in the given interval with the given boundary conditions. $\mathbf{L}^2$ is a second derivative operator like $\mathbf{K}^2$, but in the interval $0\leq x\leq b$.

It is possible, but will not be necessary here, to show a matrix form for $\mathbf{P}$. A suitable representation of $\mathbf{P}$ will be derived as follows. Let $\{\mathbf{e}(k)\}$ and $\{\mathbf{e}(l)\}$ be orthonormalized normal mode bases corresponding to guides with cross sections on $0\leq x\leq a$ and $0\leq x\leq b$, respectively. Let $\mathbf{P}\boldsymbol{E}_\tau=\boldsymbol{E}_\tau=[\boldsymbol{E}_\tau(k)]=[\boldsymbol{E}_\tau(l)]$, and define $\mathbf{T}$ as that operator required to accomplish the transformation

$$[\boldsymbol{E}_\tau(k)]=\mathbf{T}[\boldsymbol{E}_\tau(l)]. \tag{7}$$

That is, $\mathbf{T}$ gives a basis change from $\{\mathbf{e}(l)\}$ to $\{\mathbf{e}(k)\}$. Thus, except for the null-space of $\mathbf{P}$, which is to be overlooked anyway, $\mathbf{T}$ can represent $\mathbf{P}$. Like $\mathbf{P}$, $\mathbf{T}$ is a real operator. Unlike $\mathbf{P}$, $\mathbf{T}$ is not a symmetrical operator. For, on the one hand,

$$\mathbf{T}^*\mathbf{T}=\mathbf{I} \tag{8}$$

so that $\mathbf{T}^*$ retransforms from the larger to the smaller basis. On the other hand,

$$\mathbf{T}\mathbf{T}^*\neq\mathbf{I},$$

unless the domain of $\mathbf{T}^*$ consists only of functions on the iris hole; e.g., as in

$$(\mathbf{T}\mathbf{T}^*)\mathbf{T}=\mathbf{T}(\mathbf{T}^*\mathbf{T})=\mathbf{T}.$$

This property of $\mathbf{T}$ is due to the fact that, while $\mathbf{T}$ does not have a null-space, T^* does have a null-space.

There is a net advantage if $\mathbf{T}$ is used to represent $\mathbf{P}$ in (5). For then the symmetrical operator in

$$0=\mathbf{T}^*Y_l(\mathbf{K})\mathbf{T}\boldsymbol{E}_{\tau 0} \tag{9}$$

has or has not a null-space depending only on the factor $Y_l(\mathbf{K})$. Naturally, in (9), it is not necessary to insist that $\mathbf{T}\boldsymbol{E}_{\tau 0}$ (opposed to $\boldsymbol{E}_{\tau 0}$) solves the problem unless the periodic guide is actually being fed by a guide with cross-sectional width a.

If, like $\mathbf{T}$, $\mathbf{S}$ is introduced as a basis change on the iris metal, then the alternate equation (6) can be put as the more definite statement,

$$0=\mathbf{S}^*Z_l(\mathbf{K})\mathbf{S}J_{s0}. \tag{10}$$

One might note that $\mathbf{S}+\mathbf{T}$ is an orthogonal transformation, from the large guide cross section to the large guide cross section. Individually, $\mathbf{S}$ and $\mathbf{T}$ are not orthogonal. However, each might be characterized as holding some of the columns of an orthogonal matrix.

The properties of $\mathbf{T}$ help to obtain an evaluation of the operator product $\mathbf{T}^*(\mathbf{K}^2+\alpha^2)^{-1}\mathbf{T}$. It has been noted that $(\mathbf{K}^2+\alpha^2)^{-1}$ is an inverse wave operator in the larger guide, fitting zero derivative boundary conditions at the guide walls. $\mathbf{T}$ provides the functions to be operated upon (from the basis $\{\mathbf{e}(l)\}$), while $\mathbf{T}^*$ projects and transforms the result to something tractable.

In this process, what is required first is a solution to

$$\left(-\frac{\partial^2}{\partial x^2}+\alpha^2\right)F=\mathbf{e}(l), \qquad 0\leq x\leq b$$
$$=0, \qquad b\leq x\leq a, \tag{11}$$

where $\mathbf{e}(l)=\hat{x}\sqrt{\epsilon(l/b)}\cos lx$, and $\epsilon(l)=1$ when $l=0$, or $\epsilon(l)=2$ when $l>0$. With the given boundary conditions, one has

$$F=\hat{x}(l^2+\alpha^2)^{-1}\sqrt{\frac{\epsilon(l)}{b}}\cos lx - \hat{x}\sqrt{\frac{\epsilon(l)}{b}}\frac{\cos lb\cdot\sinh\alpha(a-b)}{(l^2+\alpha^2)\sinh\alpha a}\cosh\alpha x \tag{12}$$

for $0\leq x\leq b$, and

$$F=\sqrt{\frac{\epsilon(l)}{b}}\frac{\cos lb\cdot\sinh\alpha b}{(l^2+\alpha^2)\sinh\alpha a}\hat{x}\cosh\alpha(a-x) \tag{12a}$$

when $b\leq x\leq a$. Plainly, $\mathbf{T}^*F$ is given by (12).

The collection of all such $\mathbf{T}^*F$ gives a diagonal matrix for the first terms of (12), and makes a dyad[4] from the second terms of (12). Furthermore, since

$$\hat{x}\frac{\cosh\alpha x}{\alpha\sinh\alpha b}=\left[\frac{\sqrt{\frac{\epsilon(l)}{b}}\cos lb}{l^2+\alpha^2}\right] \tag{13}$$

shows a Fourier sequence representation, then one has the choice

$$\mathbf{T}^*(\mathbf{K}^2+\alpha^2)^{-1}\mathbf{T}=(\mathbf{L}^2+\alpha^2)^{-1}-\alpha\sinh\alpha b\frac{\sinh\alpha(a-b)}{\sinh\alpha a}\cdot\left[\frac{\sqrt{\frac{\epsilon(l)}{b}}\cos lb}{l^2+\alpha^2}\right]><\left[\frac{\sqrt{\frac{\epsilon(l)}{b}}\cos lb}{l^2+\alpha^2}\right] \tag{14}$$

in matrix form, or

[4] See Appendix.

$$\mathbf{T}^*(\mathbf{K}^2+\alpha^2)^{-1}\mathbf{T} = (\mathbf{L}^2+\alpha^2)^{-1} - \frac{\sinh \alpha(a-b)}{\alpha \sinh \alpha b \cdot \sinh \alpha a} \hat{x} \cosh \alpha x > < \hat{x} \cosh \alpha x \tag{14a}$$

in functional form, or a mixture if one requires it.

By using (13), changing b to d and x to z, and then evaluating at $z=0$ and $z=d$, one can write from (4):

$$Y_l(\mathbf{K}) = \frac{Y}{d} \sum_m \epsilon(m) \frac{1 - f \cos md}{\Gamma(\mathbf{K})^2 + m^2}, \tag{15}$$

which holds for $d>0$. Making use of (14a), one can put

$$\mathbf{T}^* Y_l(\mathbf{K}) \mathbf{T} = \frac{Y}{d} \sum_m \epsilon(m)(1 - f \cos md) \left\{ \frac{1}{\Gamma(\mathbf{L})^2 + m^2} - \frac{\sinh \Gamma(m)(a-b)}{\Gamma(m) \sinh \Gamma(m) b \cdot \sinh \Gamma(m) a} \cdot \hat{x} \cosh \Gamma(m) x > < \hat{x} \cosh \Gamma(m) x \right\}, \tag{16}$$

also holding for $d>0$. Thus, there is at least one general formula to give the product indicated by (9). There are others, but (16) is suitable for small d, and this will suit the sample problems to be shown.

If $\mathbf{K}^2$ in (15) and $\mathbf{L}^2$ in (16) are extended so as to mean second differentiations in the half lines below $x=a$ and $x=b$, respectively, and if x yields to the substitution $y=b-x$, then (15) can be used to show

$$\mathbf{T}^* Y_l(\mathbf{K}) \mathbf{T} = \frac{Y}{d} \sum_m \epsilon(m)(1 - f \cos md) \left\{ \frac{1}{\Gamma(\mathbf{L})^2 + m^2} - \frac{e^{-\Gamma(m)(a-b)} \sinh \Gamma(m)(a-b)}{\Gamma(m)} \hat{y} e^{-\Gamma(m) y} > < \hat{y} e^{-\Gamma(m) y} \right\}$$

for waves on a single-plane, iris-loaded guide. One must note, however, that a subset $\{0, \cdots, m_1\}$ of $\{m\}$ corresponds to outward traveling waves along y. Consequently, there is a second operator associated with (16a), having the same form, except in the replacement of outward traveling waves with inward traveling waves. Results would be the same in both cases. However, were it $a-b$ which became large instead of b, one should have pairs of solution fields (see Table I, Case III) combining to make such a guide appear as a receiving antenna, a transmitting antenna, or a power transmission line.

The operator (15) relates electric field to current density. The operator

$$K^2 Y_l(\mathbf{K}) \tag{17}$$

relates voltage field to charge density. One could let $k_0 \to 0$ in (17) and then find operators equivalent to (16) and (16a), but speaking only for static fields. Two particular effects can be mentioned: one, the $m=0$ term becomes nullified; two, the TEM waves in (16) are removed. Some further variations of the problem are shown in Table I.

TABLE I

RESULTS FOR THE E AND TEM COMBINED WAVES

	Symmetric solutions: any possible number of images about $x=0$ or $x=a$.	*Antisymmetric solutions:* only possible image pairs about $x=0$.	*Antisymmetric solutions:* only possible image pairs about $x=a$.
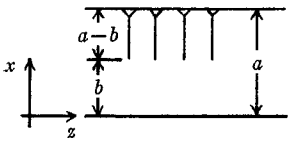 CASE I	$E_{T0}=\hat{x}\cos\sqrt{g^2+k_0^2}\,x$ $J_{s0}=\hat{x}\cos k_0(x-a)$ $k_0\tan k_0(a-b)$ $+\sqrt{g^2+k_0^2}\tan\sqrt{g^2+k_0^2}\,b=0$	$E_{T0}=\hat{x}\sin\sqrt{g^2+k_0^2}\,x$ $J_{s0}=\hat{x}\cos k_0(x-a)$ $0=k_0\tan k_0(a-b)$ $+\sqrt{g^2+k_0^2}\cot\sqrt{g^2+k_0^2}\,b$	$E_{T0}=\hat{x}\cos\sqrt{g^2+k_0^2}\,x$ $J_{s0}=\hat{x}\sin k_0(x-a)$ $k_0\cot k_0(a-b)$ $+\sqrt{g^2+k_0^2}\tan\sqrt{g^2+k_0^2}\,b=0$
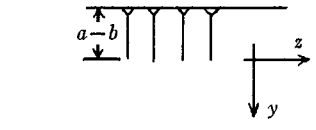 CASE II	$E_{T0}=\hat{x}e^{-\sqrt{\lvert g\rvert^2-k_0^2}\,y}$ $J_{s0}=\hat{x}\cos k_0[y-(a-b)]$ $k_0\tan k_0(a-b)-\sqrt{\lvert g\rvert^2-k_0^2}=0$		$E_{T0}=\hat{x}e^{-\sqrt{\lvert g\rvert^2-k_0^2}\,y}$ $J_{s0}=\hat{x}\sin k_0[y-(a-b)]$ $k_0\cot k_0(a-b)+\sqrt{\lvert g\rvert^2-k_0^2}=0$
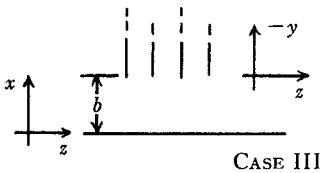 CASE III	$E_{T0}=\hat{x}\cos\sqrt{g^2+k_0^2}\,x$ $J_{s0}=\hat{x}e^{\pm jk_0 y}$ $\pm jk_0+\sqrt{g^2+k_0^2}\tan\sqrt{g^2+k_0^2}\,b=0$	$E_{T0}=\hat{x}\sin\sqrt{g^2+k_0^2}\,x$ $J_{s0}=\hat{x}e^{\pm k_0 y}$ $\pm jk_0+\sqrt{g^2+k_0^2}\cot\sqrt{g^2+k_0^2}\,b=0$	
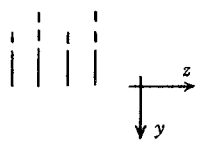 CASE IV	$E_{T0}=\hat{x}e^{\pm jk_0 y}$ $J_{s0}=\hat{x}e^{\pm jk_0 y}$ $g=h=0$		

IV. Solution Procedure

When d is small, (16) can become simplified; i.e., when $k_0 d$ is small, say $k_0 d \leq 0.1\pi$. The total phase shift per cell is not necessarily so limited, for it will be seen that the dimensions a and b can be chosen from a large set of possible values. It was mentioned that results will be shown which would extend the range of usefulness of some known formulas and curves. Indeed, when multimode guides are considered, one might think any contribution to accuracy of results is helpful. Some tests on the following sample problem will show that, as $|hd|$ varies from 0 to π, error in $|hd|$ rises to five percent off the values required for solving (9).

Some inaccuracies in the next few lines will need to be refined when the reasons for them are shown. Put (15) in the form

$$\frac{2}{f+1} Y_l(\mathbf{K}) = Y_0(\mathbf{K}) \left[\tanh \frac{1}{2} \Gamma(\mathbf{K}) d - \frac{f-1}{f+1} \coth \frac{1}{2} \Gamma(\mathbf{K}) d \right] \quad (18)$$

so that as $d \to 0$

$$\frac{g^2 d}{Y(f-1)} Y_l(\mathbf{K}) \sim 1 - g^2 \frac{1}{\Gamma(\mathbf{K})^2}; \quad (19)$$

wherein the replacements

$$\frac{2}{\Gamma(\mathbf{K}) d} \tanh \frac{1}{2} \Gamma(\mathbf{K}) d \doteq 1 \quad (20)$$

and

$$\frac{2}{\Gamma(\mathbf{K}) d} \coth \frac{1}{2} \Gamma(\mathbf{K}) d \doteq \frac{4}{\Gamma(\mathbf{K})^2 d^2} + \frac{1}{3} \quad (21)$$

have been made, and where

$$g^2 = \frac{4}{d^2} \left(\frac{f-1}{f+1} \right) \left[1 - \frac{1}{3} \left(\frac{f-1}{f+1} \right) \right]^{-1} = \frac{4}{d^2} \sinh^2 \frac{h_1 d}{2} \left[1 + \frac{2}{3} \sinh^2 \frac{h_1 d}{2} \right]^{-1}. \quad (22)$$

The notation h_1 is meant to suggest that h_1 can stand correction. Note that in (22) the constraint $-12 \leq g^2 d^2 \leq 6$ for all real or imaginary h; and note also the poles of g^2 located at

$$\pm h_1 = d^{-1} \sinh^{-1} \frac{\sqrt{2}}{2} + j d^{-1} \pi (2t+1),$$

where t can be any positive or negative integer. One can see that the waveguide problem would be characterized more accurately by (19) the further out the poles are placed, implying that accuracy is favored when $|h_1 d|$ is small. If $|h_1 d| \leq 0.30\pi$, then

$$g^2 \doteq \frac{h_1^2}{1 + \frac{1}{6} h_1^2 d^2} \doteq h_1^2 (1 - \tfrac{1}{6} h_1^2 d^2) \quad (22a)$$

can be used to replace (22).

Now, taking (19) to be an estimate of (15), let (16) be estimated by

$$\frac{g^2 d}{Y(f-1)} \mathbf{T}^* Y_l(\mathbf{K}) \mathbf{T} \sim 1 - g^2 \frac{1}{\Gamma(\mathbf{L})^2} - \frac{g^2 \sin k_0 (a-b)}{k_0 \sin k_0 b \cdot \sin k_0 a} \hat{x} \cos k_0 x > < \hat{x} \cos k_0 x \quad (23)$$

when $d \to 0$. Upon operating on the left sides of the operators in (23) with $\Gamma(\mathbf{L})^2 (\Gamma(\mathbf{L})^2 - g^2)^{-1}$, one obtains

$$1 - \frac{g^2 \sin k_0 (a-b)}{\sqrt{k_0^2 + g^2} \sin \sqrt{k_0^2 + g^2}\, b \cdot \sin k_0 a} \cdot \hat{x} \cos \sqrt{k_0^2 + g^2}\, x > < \hat{x} \cos k_0 x. \quad (24)$$

Since $\boldsymbol{E}_{\tau 0}$ is the null-space of (24), one has immediately that

$$\boldsymbol{E}_{\tau 0} = \hat{x} \cos \sqrt{k_0^2 + g^2}\, x. \quad (25)$$

$\boldsymbol{E}_{\tau 0}$ is finite at the iris edge in (25), but this can still be a fair representation of electric field in the iris hole since the infinite rise of $\boldsymbol{E}_{\tau 0}$ should start nearer the edge and pass a smaller fraction of power, as $d \to 0$. If the set of irises is taken as an artificial dielectric insert, then (25) shows a field whose magnitude drops off in an expected manner, away from the interface of free space with a dielectric insert, when $k_0^2 + g^2 < 0$.

One can calculate as a check on $\boldsymbol{E}_{\tau 0}$, corresponding to each term in (16), the value of the quadratic form

$$(\boldsymbol{E}_{\tau 0}, \mathbf{T}^* (\Gamma(\mathbf{K})^2 + m^2)^{-1} \mathbf{T} \boldsymbol{E}_{\tau 0}) \doteq \frac{1}{m^2 - k_0^2} - \frac{\sqrt{|g|^2 - k_0^2}}{(m^2 - k_0^2)(\sqrt{m^2 - k_0^2} + \sqrt{|g|^2 - k_0^2})}; \quad (26)$$

and it is now implicit that $k_0^2 + g^2 < 0$. If a sum[5] is made over $\{m_e > 0\}$, one finds that

$$2 \sum_{m_e > 0} \frac{(\boldsymbol{E}_{\tau 0}, \mathbf{T}^* (\Gamma(\mathbf{K})^2 + m^2)^{-1} \mathbf{T} \boldsymbol{E}_{\tau 0}}{(E_{\tau 0}, \mathbf{T}^* \Gamma(\mathbf{K})^{-2} \mathbf{T} \boldsymbol{E}_{\tau 0})} \doteq 2 \left(\frac{gd}{2\pi} \right)^2 \left[0.629 - 0.185 \frac{\sqrt{|g|^2 - k_0^2 d}}{2\pi} + \frac{1}{1 + \sqrt{|g|^2 - k_0^2}\, \frac{d}{2\pi}} \right]. \quad (27)$$

[5] L. B. W. Jolley, *Summation of Series*, 2nd rev. ed. New York: Dover, 1961, pp. 62–65, 240–242.

Thus, when $k_0 d < |gd| = 0.2\pi$, (27) shows a three-percent error in the estimate (23) of (16) due to operators with index $m_e > 0$. At the same time, if (26) is summed[5] over $\{m_0\}$, one should have

$$8 \sum_{m_0} \frac{(\boldsymbol{E}_{\tau 0}, \mathbf{T}^*(\Gamma(\mathbf{K})^2 + m^2)^{-1}\mathbf{T}\boldsymbol{E}_{\tau 0})}{(\boldsymbol{E}_{\tau 0}, \mathbf{T}^*\Gamma(\mathbf{K})^{-2}\mathbf{T}\boldsymbol{E}_{\tau 0})} \doteq 8\left(\frac{gd}{\pi}\right)^2 \left[0.221 - 0.043\sqrt{|g|^2 - k_0^2}\,\frac{d}{\pi} + \frac{1}{1 + \sqrt{|g|^2 - k_0^2}\,\dfrac{d}{\pi}}\right]. \quad (28)$$

By contrast with (27), (28) shows a 14-percent error in the estimate of (16) by (23) due to terms indexed m_0, for the condition $|gd| = 0.2\pi$. If the region of iris metal were smaller, then the dyads in (16) and (23) would have smaller amplitudes, yielding $\sqrt{|g|^2 - k_0^2}$ more nearly zero; so that (26) should have more nearly the form $(m^2 - k_0^2)^{-1}$, yielding in turn more nearly zero errors in the tests (27) and (28). Therefore, it is chiefly the size of iris metal that may cause error in using (23) to represent the waveguide problem when d is small.

Nevertheless, it appears the estimates (19), (23), and (25) are really quite useful. For what is needed, in view of (27) and (28), is only to change the replacements (20) to

$$\frac{2}{\Gamma(\mathbf{K})d} \tanh \frac{1}{2}\Gamma(\mathbf{K})d \doteq g_1 = \frac{8}{\pi^2}\left[0.221 - 0.043\sqrt{|g|^2 - k_0^2}\cdot\frac{d}{\pi} + \frac{1}{1 + \sqrt{|g|^2 - k_0^2}\,\dfrac{d}{\pi}}\right], \quad (29)$$

and (21) to

$$\frac{2}{\Gamma(\mathbf{K})d} \coth \frac{1}{2}\Gamma(\mathbf{K})d = \frac{4}{\Gamma(\mathbf{K})^2 d^2} + g_2, \quad (30)$$

where

$$g_2 = \frac{2}{\pi^2}\left[0.629 - 0.185\sqrt{|g|^2 - k_0^2}\,\frac{d}{2\pi} + \frac{1}{1 + \sqrt{|g|^2 - k_0^2}\,\dfrac{d}{2\pi}}\right]; \quad (30a)$$

and consequently also changing (22) to

$$g^2 = \frac{4}{d^2}\left(\frac{f-1}{f+1}\right)\left[g_1 - \left(\frac{f-1}{f+1}\right)g_2\right]^{-1}, \quad (31)$$

as well as the simpler form (22a) to

$$g^2 \doteq \frac{h^2}{g_1}\left[1 - \frac{g_1 - g_2}{4g_1}h^2 d^2\right] \doteq \frac{h^2}{g_1}\left(1 - \frac{1}{6}h^2 d^2\right). \quad (31a)$$

One should now find that corrections $\Delta\boldsymbol{E}_{\tau 0}$ on $\boldsymbol{E}_{\tau 0}$ of (25), such that $\|\Delta\boldsymbol{E}_{\tau 0}\|_1 = 0.1\|\boldsymbol{E}_{\tau 0}\|_1$, would produce first-order variations in

$$\frac{\left(\boldsymbol{E}_{\tau 0}, \mathbf{T}^*\Gamma(\mathbf{K})^{-1}\coth\Gamma(\mathbf{K})\dfrac{d}{2}\mathbf{T}\boldsymbol{E}_{\tau 0}\right)}{\left(\boldsymbol{E}_{\tau 0}, \mathbf{T}^*\Gamma(\mathbf{K})^{-1}\tanh\Gamma(\mathbf{K})\dfrac{d}{2}\mathbf{T}\boldsymbol{E}_{\tau 0}\right)} \quad (32)$$

[using (26), (27), and (28)] that are not greater than second-order variations. This confirms the stationary character of (32) near $\boldsymbol{E}_{\tau 0}$.

The condition for no inverse to (24) is found [see Appendix (49)] by forming the inner product expression

$$A(\hat{x}\cos k_0 x, \boldsymbol{E}_\tau)$$

of (24) with arbitrary $\boldsymbol{E}_\tau$ and with $\hat{x}\cos k_0 x$; wherein

$$A = 0 = 1 - \frac{g^2 \sin k_0(a-b)}{\sqrt{k_0^2 + g^2}\sin\sqrt{k_0^2 + g^2}\,b \cdot \sin k_0 a} \cdot \int_0^b \cos k_0 x \cos\sqrt{k_0^2 + g^2}\,x dx.$$

A can be rearranged to show a simpler statement,

$$0 = k_0 \tan k_0(a-b) + \sqrt{k_0^2 + g^2}\tan\sqrt{k_0^2 + g^2}\,b, \quad (33)$$

of the condition for fields (25) in the periodic waveguide when d is small. Thus, g is found from (33), $\boldsymbol{E}_{\tau 0}$ from (25), and finally h from (31) or (31a).

V. Results

Table I lists results for several periodic guide configurations, more or less easily derivable from the case just considered by the process just shown. The use of relation (31) or (31a) for determining h from g in each case is presumed. The relation (4), to give J_{s0} from $\boldsymbol{E}_{s0}$, is also presumed. This can make use of the approximate operator

$$Y_l(\mathbf{K}) \doteq Y\left[(f+1)\frac{g_1 d}{4} - (f-1)\frac{g_2 d}{4} - \frac{f-1}{d}\frac{1}{\Gamma(\mathbf{K})^2}\right], \quad (34)$$

where $\Gamma(\mathbf{K})^{-2}$ makes use of an appropriate finite or infinite range representation; e.g., as in (16) and (16a).

The symmetric solution, Case I, corresponds to the problem just worked. Symmetric solutions, where possible, are obtained by first rotating the planar waveguide about $x=0$ or $x=a$, and then continuing the symmetric Case I solution to cover the combined region. Thereafter, in Case I, any further number of such images can be added to that just shown. The imaging process stops after the first one in Cases II and III. Case IV allows no imaging process. Evidently, the suggestion of actual symmetry is false when the number of images is odd.

If the sample problem were worked for the case of a guide with two symmetric iris metallic regions or two symmetric iris holes, one should find each such iris configuration to allow two solutions: one, a symmetric solution; two, what can be called an antisymmetric solution. The antisymmetric solutions in Table I, therefore, correspond only to even numbers of images of the guide being considered.

As the number of images increases, the Case I antisymmetric solutions tend to disappear. On the other hand, the symmetric solutions approach a limiting behavior which can be characterized by

$$-g^2 \to k_0^2 \frac{a}{b};$$

the ratio of conducting domain width to nonconducting domain width giving relative permittivity for this limiting artificial dielectric.

When an image is taken around $x=a$, as it may in Cases I and II, and if symmetric and antisymmetric solutions are combined, then the resultant guide exhibits directional coupler (or re-entrant wave) action. That is, both fields do not propagate simultaneously, so that (when one of them does) their sum shows a transfer of some power from one set of iris holes through the artificial dielectric to the other set of holes. Similar action occurs when imaging is done around $x=0$, as in Cases I and III, but power transfer is made from one side to the other of just one set of iris holes.

The Case III is peculiar for two further reasons. On the one hand, the propagation constant is complex. This is due to the assumed infinite width of the guide, requiring an implicit source (or sink) at $x=\infty$. Compare Case II; this does not happen to be the effect there except when $g=0$. As one might expect when g is complex, there are four symmetric and four antisymmetric propagation constants for the guide of Case III. One could, if one wished, combine these waves to produce purely x directed propagation, or a form of purely z directed propagation, although this is not a necessary task, since all the power in these guides is accounted for.

On the other hand, because of the right angle turn of the wave in the Case III guides, one has a detail picture of re-entrant (or directionally coupled) wave action due to a source at $x=\infty$. Case IV provides a view of the source at infinity.

The guide can be looked upon as containing diamagnetic material when H waves are present, and does not give rise to slow waves. Without further comment, H-wave results corresponding to Case I are listed below:

1) Antisymmetrically imaged:

$$\left.\begin{aligned} &\frac{\sqrt{h^2+k_0^2}}{\sqrt{g_3^2+h^2+k_0^2}} \cot \sqrt{h^2+k_0^2}\, b + \cot \sqrt{g_3^2+h^2+k_0^2}\,(a-b) = 0 \\ &E_{\tau 0} = \hat{y} \sin \sqrt{h^2+k_0^2}\, x \\ &J_{s0} = \hat{y} \sin \sqrt{g_3^2+h^2+k_0^2}\,(a-x). \end{aligned}\right\} \tag{34}$$

2) Symmetrically imaged:

about $x=0$

$$\left.\begin{aligned} E_{\tau 0} &= \hat{y} \cos \sqrt{h^2+k_0^2}\, x \\ J_{s0} &= \hat{y} \sin \sqrt{g_3^2+h^2+k_0^2}\,(a-x) \end{aligned}\right\} \text{ and } \tan \sqrt{g_3^2+h^2+k_0^2}\,(a-b) + \frac{\sqrt{h^2+k_0^2}}{\sqrt{g_3^2+h^2+k_0^2}} \cot \sqrt{h^2+k_0^2}\, b = 0$$

about $x=a$

$$\left.\begin{aligned} E_{\tau 0} &= \hat{y} \sin \sqrt{h^2+k_0^2}\, x \\ J_{s0} &= \hat{y} \cos \sqrt{g_3^2+h^2+k_0^2}\,(a-x) \end{aligned}\right\} \text{ and } \cot \sqrt{g_3^2+h^2+k_0^2}\,(a-b) + \frac{\sqrt{h^2+k_0^2}}{\sqrt{g_3^2+h^2+k_0^2}} \tan \sqrt{h^2+k_0^2}\, b = 0 \tag{35}$$

In both (34) and (35),

$$-g_3^{-2} = \frac{1}{h^2+k_0^2} - \frac{d}{2\sqrt{h^2+k_0^2}} \cot \frac{1}{2} \sqrt{h^2+k_0^2}\, d. \tag{36}$$

As $d \to 0, -g_3^2 \backsim (d^2/12)$.

VI. Additional Error Checks

There is reason to state that the results (25), (31), (31a), and (33) are relatively good ones—in the sense of practical convenience—when the designer is also the calculator. In order to illustrate this, consider a two-term approximation to (15); i.e., the operator estimate

$$\left[1 - \frac{f-1}{f+1}\frac{1}{3} - \frac{4}{d^2}\frac{f-1}{f+1}\frac{1}{\Gamma(\mathbf{K})^2}\right] + \left[\frac{8}{d^2}\frac{1}{\Gamma(\mathbf{K})^2 + \left(\frac{\pi}{d}\right)^2} - \frac{8}{\pi^2}\right]. \quad (37)$$

If one uses the uncorrected g^2, formula (22), then

$$2\,\frac{f+1}{f-1}\left(\frac{gd}{\pi}\right)^2 \frac{\Gamma(\mathbf{L})\left[1 - 2\left(\frac{gd}{\pi}\right)^2\left(\frac{f+1}{f-1}\right)\right] + \Gamma(\mathbf{L})^2\left[\left(\frac{\pi}{d}\right)^2 - g^2\right] - g^2\left(\frac{\pi}{d}\right)^2}{\Gamma(\mathbf{L})^2\left[\Gamma(\mathbf{L})^2 + \left(\frac{\pi}{d}\right)^2\right]} \quad (38)$$

corresponds, as an approximation, to the diagonal terms of (16). In this process, similar to that used for finding (25), the roots γ_1^2 and γ_2^2 of the numerator in (38) will produce the functions $\cos\sqrt{\gamma_1^2+k_0^2}x$ and $\cos\sqrt{\gamma_2^2+k_0^2}x$—linear combinations of which are required to represent $\boldsymbol{E}_{\tau 0}$. The roots can be found from

$$\left(\frac{g}{\gamma}\right)^2 = -\frac{1}{2}\left[1 - \left(\frac{gd}{\pi}\right)^2\right] \pm \frac{1}{2}\sqrt{\left[1 + \left(\frac{gd}{\pi}\right)^2\right]^2 - 8\left(\frac{f+1}{f-1}\right)\left(\frac{gd}{\pi}\right)^4}. \quad (39)$$

γ_1 and γ_2 have, at most, the same order of magnitude (around $hd = 150°$), but are never, even approximately, equal. Say that $|\gamma_1|$ is less than $|\gamma_2|$. Then γ_1 will adjust the power content of $\boldsymbol{E}_{\tau 0}$ and γ_2 the field rise at the iris edge.

When $|hd|$ is small, $\boldsymbol{E}_{\tau 0}$ is powerful over much of the iris hole. When $|hd|$ is large, there is power only near the iris edge. Thus, when $|hd|$ is small, it is a measure of comparison between the operators (37) and (19) that the corrected $g^2 \doteq \gamma_1^2$; and when $|hd|$ is large, that the corrected $g^2 \doteq \gamma_2^2$.

Assuming $|hd| \doteq 80°$, one finds

$$\left(\frac{g}{\gamma}\right)^2 \doteq -\frac{1}{2}\left[1 - \left(\frac{gd}{\pi}\right)^2\right] \pm \frac{\sqrt{2}}{2}\left[1 + \left(\frac{gd}{\pi}\right)^2\right],$$

which yields $|\gamma_2|^2 \doteq 20|\gamma_1|^2$ and $|\gamma_1|^2$ about 1.0 percent off the magnitude of the corrected g^2. Assuming $|hd| \doteq 150°$, one finds

$$\left(\frac{g}{\gamma}\right)^2 \doteq \frac{1}{2}\left[1 - \left(\frac{gd}{\pi}\right)^2\right] \pm \sqrt{2}\left(\frac{gd}{\pi}\right)^2\sqrt{-\frac{f+1}{f-1}},$$

which yields $|\gamma_2|^2 \doteq 2|\gamma_1|^2$ and γ_2^2 about 10 percent off in magnitude of the corrected g^2. The cause of this difference might be laid to the incompletely diminished power due to γ_1. The percent difference is even larger when $|hd| = \pi$, for the reason that higher m_e index terms in (15) come into effectiveness. In this case, more accurate results obtain when the corrected g^2 is used, instead of γ^2, to show the field function. Indeed, for a two m_e term approximation at $|hd| = \pi$, one finds the corrected g^2 about 10 percent above γ^2; the difference tending to diminish as higher m_e terms are included in the estimate of the operator.

VII. The Interdigital Periodic Line

For an additional sample problem, consider the interdigital line shown in Fig. 2. The same dielectric medium is used here as in Fig. 1. One finds, corresponding to (3), that

$$\begin{pmatrix} \hat{z} \times \boldsymbol{H}_{\tau 01} \\ e^{-hd_z} \times \boldsymbol{H}_{\tau 02} \end{pmatrix} = Y_0(\mathbf{K}) \begin{pmatrix} \coth \Gamma(\mathbf{K})d & -e^{hd}\operatorname{csch}\Gamma(\mathbf{K})d \\ -e^{hd}\operatorname{csch}\Gamma(\mathbf{K})d & \coth\Gamma(\mathbf{K})d \end{pmatrix} \begin{pmatrix} \boldsymbol{E}_{\tau 01} \\ e^{-hd}\boldsymbol{E}_{\tau 02} \end{pmatrix} = \underline{Y_i(\mathbf{K})} \begin{pmatrix} \boldsymbol{E}_{\tau 01} \\ e^{-hd}\boldsymbol{E}_{\tau 02} \end{pmatrix}. \quad (40)$$

The multimatrix form $\underline{Y_i(\mathbf{K})}$ of the iterative admittances is convenient because of the distinctiveness of each iris in the pair considered. Corresponding to (4), one finds that

$$\begin{pmatrix} J_{s01} \\ e^{-hd}J_{s02} \end{pmatrix} = 2Y_0(\mathbf{K}) \begin{pmatrix} \coth \Gamma(\mathbf{K})d & -f\operatorname{csch}\Gamma(\mathbf{K})d \\ -f\operatorname{csch}\Gamma(\mathbf{K})d & \coth\Gamma(\mathbf{K})d \end{pmatrix} \begin{pmatrix} \boldsymbol{E}_{\tau 01} \\ e^{-hd}\boldsymbol{E}_{\tau 02} \end{pmatrix} = 2\underline{Y_i(\mathbf{K})} \begin{pmatrix} \boldsymbol{E}_{\tau 01} \\ e^{-hd}\boldsymbol{E}_{\tau 02} \end{pmatrix}, \quad (41)$$

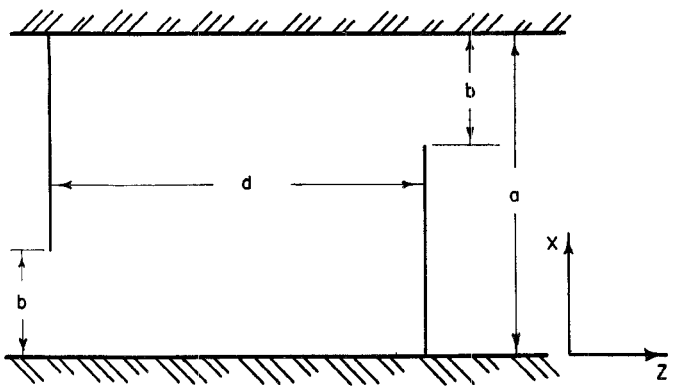

Fig. 2. The interdigitally loaded planar waveguide. Its properties differ from those in Fig. 1 only in the conductor boundary configuration.

where $2Y_l(\mathbf{K})$ is the multimatrix loading admittance, and f is still given by (4a). Here, the statement equivalent to (9) is

$$0 = \begin{pmatrix} \mathbf{T}_1^* & 0 \\ 0 & \mathbf{T}_2^* \end{pmatrix} \underline{Y_l(\mathbf{K})} \begin{pmatrix} \mathbf{T}_1 & 0 \\ 0 & \mathbf{T}_2 \end{pmatrix} \begin{pmatrix} E_{\tau 01} \\ e^{-hd}E_{\tau 02} \end{pmatrix}, \quad (42)$$

$\mathbf{T}_1$ and $\mathbf{T}_2$ being respective realizations of projection on successive irises.

If one uses the information, due to translational symmetry, that

$$E_1(x, z) = \pm e^{-hd}E_2(x - a, z + d), \quad (43)$$

then (42) can be rearranged to fit either (for either mode) of the simpler statements

$$0 = \mathbf{T}^* Y_0(\mathbf{K})[\coth \Gamma(\mathbf{K})d \mp f \operatorname{csch} \Gamma(\mathbf{K})d]\mathbf{T}E_{\tau 01}; \quad (44)$$

where the indication $\mp$ in (44) matches $\pm$ in (43), and where $\mathbf{T}$ is as defined for the preceding sample problem. The signs $\mp$ in (44) also match the choice hd or $hd+j\pi$ for phase shift. Thus, the formal consideration of the interdigital line is like that of the periodic line: Table I and other formulas and curves[1,2] of the periodic line apply to both lines. Indeed, so long as $2d$ is iris periodicity, this last remark applies to both the thin- and the thick-iris loaded guides.

The corrected g^2 (31) is needed to solve (44), but one must distinguish between corrections needed for one or the other case in (44). It is not simply (though it may usually be) that the correction depends on whether hd deviates from 0 or from $j\pi$, or not.

A noteworthy point derived from the double statement (44) lies in the fact that there can be slow H waves here; i.e., corresponding to a slow fundamental space (Hartree) harmonic.

VIII. Concluding Remarks

The series representation (15) of the loading admittance operator requires that more terms be used when iris separation increases. When d is sufficiently large, one could choose to replace (15) by a series such that fewer terms are required for approximation. Thus the admittance operator representation needs to be chosen to suit conditions on the waveguide. It is not digressive, furthermore, to suggest that the approach made here can (for the appropriate operators) be used in the treatment of other loadings, such as the single iris and the thick (single, periodic, or interdigitally placed) iris.

Appendix

Let u and v be vectors in the same finite or infinite dimensional space. Then the calculations uv^* and v^*u can each exist. One says conventionally[6] that

$$uv^* = u > < v, \quad (45)$$

which is an operator called a dyad; and that

$$v^*u = (v, u) = \langle v, u \rangle, \quad (46)$$

a scalar product. The alternative scalar product notation is suggestive when forming dyad products like $u_1 > < v_1 u_2 > < v_2 = (v_1, u_2)u_1 > < v_2$. Given an operator of the form

$$1 + u > < v, \quad (47)$$

its inverse has the form

$$1 - \frac{u > < v}{1 + (v, u)}. \quad (48)$$

This property can be used to give a sequential display of the inversion of operators like

$$1 + \sum_t u_t > < v_t.$$

The condition for no inverse (48) to (47) is seen to be

$$1 + (v, u) = 0. \quad (49)$$

In general, truncation of a large set of linear equations corresponds to termination of a series of dyads. There can sometimes be a net advantage in the use of dyads to depict favorable coordinate axes transformations.

Acknowledgment

Support of this work by the U. S. Army Research Office (Durham) is gratefully acknowledged.

[6] B. Friedman, *Principles and Techniques of Applied Mathematics*. New York: Wiley, 1956.